

CrossMark
click for updatesCite this: *RSC Adv.*, 2014, 4, 38797

Electromagnetic interference shielding properties of solid-state polymerization conducting polymer†

Fan Wu,* Zhuanghu Xu, Yuan Wang and Mingyang Wang*

Poly(3,4-ethylenedioxythiophene) (PEDOT) has been synthesized through a facile solid-state polymerization (SSP) approach. The polymerization was simply initiated by sintering the monomer, 2,5-dibromo-3,4-ethylenedioxythiophene (DBEDOT), at a temperature of 80 °C. A high performance shield for electromagnetic interference (EMI) protection based on this SSP-PEDOT has been developed. The SSP-PEDOT with a heating time of 24 hours has the maximum value of the dielectric loss tangent ($\tan \delta_d$) in the frequency range of 2–18 GHz, which revealed that this sample has the best electromagnetic energy absorption ability. When the thickness of the sample reached 2 mm, the bandwidth with the reflection loss (RL) deeper than -10 dB was nearly 5.9 GHz (from 10.0 GHz to 15.9 GHz), and the maximum value of RL was about -50.1 dB at 11.2 GHz. The SSP-PEDOT with a heating time of 1 hour had the best EMI shielding effectiveness (SE_{total}) in the entire frequency range of 2–18 GHz, which was almost contributed to the reflection from the material surface (SE_R). These results demonstrated that SSP initiated at low temperature shows multi-practical EMI shielding application in the areas of military camouflage and electronic devices protection.

Received 5th June 2014
Accepted 1st August 2014

DOI: 10.1039/c4ra05340k

www.rsc.org/advances

Introduction

Electromagnetic pollution has become a serious danger all over the modern world. Electromagnetic interference (EMI) can lead to harmful effects on electronic devices as well as organisms, and therefore human beings should keep away from the hazards of the wide use of commercial, military, and scientific electronic equipment. Increasing attention has been given to the preparation of EMI shielding materials. The conventional EMI shielding materials are based on metal films or plates; although they have a good EMI shielding effectiveness (SE), they have some drawbacks including usability problems, such as heavy weight, corrosion, poor processibility, and their EMI shielding mechanism (electromagnetic reflection) limits their future applications.^{1,2} Nowadays, considerable effort has been made for the development of new types of EMI shielding materials with the properties of high-performance EMI SE, lightweight and flexible.³

Lightweight is a key for the next generation EMI shielding materials for use in the areas of aircraft, spacecraft, and automobiles because it would save material, energy, and space. Recently, electrically conductive materials, such as carbon nanotubes (CNTs),^{4,5} reduced graphene oxide (RGO),^{6,7} and intrinsically conducting polymers (ICPs),^{2,8–10} have received

significant attention for EMI shielding applications. CNTs and RGO have been used as conductive fillers to fabricate materials for EMI shielding because of high electrical conductivity, excellent mechanical properties, lightweight, flexibility, and large aspect ratio.^{3–7} For example, Li *et al.*⁴ prepared an epoxy composite with 15 wt% single-walled CNTs, reaching an SE of around 15–20 dB in the 500 MHz to 1.5 GHz range. Yang *et al.*⁵ reported a polystyrene/multi-walled CNTs composite, which has 20 dB of SE in the frequency range of 8.2–12.4 GHz (X band). RGO is an extensively studied material in current research, and it has a potential of EMI shielding. Hsiao *et al.*⁶ prepared the polyurethane/RGO for EMI shielding with a SE of more than 30 dB at X band. Shen *et al.*⁷ reported an EMI SE of 18 dB (X-band) through polyetherimide/RGO@Fe₃O₄ foams. Although carbon based nanofillers display extremely low percolation thresholds, they are costly, are difficult to produce on a large scale and often need complicated purification/functionalization steps.⁹ In this context, ICPs are more attractive materials due to their lightweight, versatility, low cost, and processibility. Among the available ICPs, polyaniline (PANI) based materials used in EMI shielding have been reported for years.^{2,8,9} The effect on thickness,² crystal size,⁸ and doping materials⁹ in EMI SE has been completely studied. Liu *et al.*¹¹ reported that PEDOT-reduced GO-Co₃O₄ composites RL can reach -51.1 dB at 10.7 GHz, and the bandwidth exceeding -10 dB is 3.1 GHz with an absorber thickness of 2.0 mm.

PEDOT was first synthesized in the early 1990s;¹² because of its excellent electronic properties and high stability, PEDOT is one of the most industrially important conjugated

State Key Laboratory for Disaster Prevention & Mitigation of Explosion & Impact, PLA University of Science and Technology, Nanjing 210007, P. R. China. E-mail: wufanjlg@163.com; wmyrf@163.com; Tel: +86 25 80825361

† Electronic supplementary information (ESI) available. See DOI: 10.1039/c4ra05340k

polymers.^{13–15} The idea of solid-state polymerization (SSP) of suitable monomers with a well-ordered crystalline structure was realized in the 1960s and 1970s with polydiacetylenes¹⁶ and (SN)_x.¹⁷ After that, SSP has been widely used in the preparation of polycrystalline solids^{18,19} and conducting polymers^{20,21} with the advantages of environmental friendliness and relatively high yields. In 1996, Sotzing *et al.*²² first reported a method to synthesize 2,5-dibromo-3,4-ethylenedioxythiophene (DBEDOT) through bromination. In 2003, Meng *et al.*²⁰ fully studied the SSP mechanism of PEDOT through halogenation (Cl, Br, I). They found that crystalline DBEDOT affords a highly conducting monomer only through gentle heating.

SSP is a catalyst-free cross-coupling reaction without solvent, and it is a facile method for the polymerization of suitable monomer species.^{20,21} SSP of well-ordered halogenated crystalline heterocyclic monomers can yield highly conductive polymers. According to these advantages, we have already using the SSP-PEDOT as Pt-free counter electrodes (CEs) for dye-sensitized solar cells (DSSCs).²³ In the present study, we report that SSP-PEDOT has high performance in EMI protection *via* DBEDOT as the monomer. The polymerization reaction was simply carried out by heating at low temperature without the addition of any catalysts, leading to the formation of the high yield SSP-PEDOT. The SSP-PEDOT with different heating times give completely different EMI mechanisms, which are favorable for multi-practical EMI shielding applications in the areas of military camouflage, and electronic devices protection.

Experimental section

Materials

3,4-Ethylenedioxythiophene, *N*-bromosuccinimide were purchased from Adamas-beta, Titan Scientific Co., Ltd, Shanghai, China. Glacial acetic acid, methylene chloride (CH₂Cl₂), petroleum ether were purchased from GENERAL-REAGENT, Titan Scientific Co., Ltd, Shanghai, China. Chloroform was supplied by Professor Wei Dong, Nanjing University of Science & Technology, China. Distilled water was obtained from a Direct-Q3 UV, Millipore.

Synthesis of 2,5-dibromo-3,4-ethylenedioxythiophene (DBEDOT)

2,5-Dibromo-3,4-ethylenedioxythiophene (DBEDOT) monomer was synthesized according to the previous reports with minor modifications.^{20,22} In brief, 6.0 g of 3,4-ethylenedioxythiophene (EDOT) was first mixed in a solution of 100.0 mL of CHCl₃ and 100.0 mL of glacial acetic acid. Then, 16.0 g of *N*-bromosuccinimide was slowly added to the abovementioned solution at 0–5 °C under an Ar atmosphere. After stirring for 5 hours, the solution was poured into 200 mL of distilled water. The green-blue organic layer was separated, and the water layer was extracted with CHCl₃ (50 mL × 3). The combined organic layer was washed with distilled water several times. The solvent was then removed under vacuum by rotary evaporation. The dark blue solid product was purified using column chromatography with CH₂Cl₂ and petroleum ether (1 : 1) as the eluent to obtain

white crystals in 75% yield (9.5 g). ¹H NMR (CDCl₃): (4.4 ppm, s, CH₂). ¹³C NMR (CDCl₃): 140.3, 84.6, 65.1 ppm.

Synthesis of SSP poly(3,4-ethylenedioxythiophene) (SSP-PEDOT)

The white crystals of DBEDOT were first grinded into a powder. 400 mg of this powder was placed into a 20 mL glass bottle. Then, the bottle was put into a vacuum oven at 80 °C. Heating the DBEDOT monomer at this temperature can produce a highly conducting polymer film, according to previous reports.²⁰ After SSP for 1 hour, the color of the powder turned to dark blue, and the SSP-PEDOT was obtained. The bottle was then kept at room temperature and flushed under an Ar atmosphere for 30 min to remove elemental bromine (Br₂). Other samples were obtained in the same manner but the SSP times were different and included 2, 4, 8, 12, 24, 48 hours.

Characterization and measurement

The detailed morphologies of the DBEDOT monomer and PEDOT were observed with a field emission scanning electron microscope through spin-coating on to a slide (FE-SEM, S4800, Hitachi). X-ray photoelectron spectroscopy (XPS) was carried out in a Thermo Scientific ESCALAB 250Xi X-ray photoelectron spectrometer equipped with an amonochromatic Al K α X-ray source (1486.6 eV). The molecular weight of the polymers were measured by the gel permeation chromatography (GPC) method at 40 °C, and polystyrene was used as a standard by using chloroform as the eluent at a flow rate of 1.0 mL min⁻¹. Differential scanning calorimetry (DSC) was performed on a DSC 823e (Mettler Toledo) with a heating rate of 10 °C min⁻¹ under a nitrogen flow. Thermogravimetric analysis was carried out on a TGA/SDTA 851e (Mettler Toledo) at a heating rate of 10 °C min⁻¹ under nitrogen and atmosphere. For electromagnetic shielding measurements an Agilent N5242A PNA-X vector network analyzer in the frequency range of 2–18 GHz was used. The measured samples were prepared by uniformly mixing 50 wt% of the sample with a paraffin matrix at 100 °C. The mixture was then pressed into toroidal shaped samples with an outer diameter of 7.00 mm and inner diameter of 3.04 mm.

Theory of electromagnetic interference shielding

The EMI SE of a material can be defined as the ratio of transmitted power to incident power,²⁴ and it is considered to be the sum of reflection from the material surface (SE_R), absorption of electromagnetic energy (SE_A), and multiple internal reflections (SE_M) of electromagnetic radiation (Fig. 1). Because the frequency range is from 2–18 GHz, the source-to-shield distance should be greater than the free-space wavelength, so that the measurements are considered under far field.²⁴ It can be expressed as^{3–7,24}

$$SE_{\text{total}} = 10 \lg \left(\frac{P_1}{P_0} \right) = SE_A + SE_R + SE_M \quad (1)$$

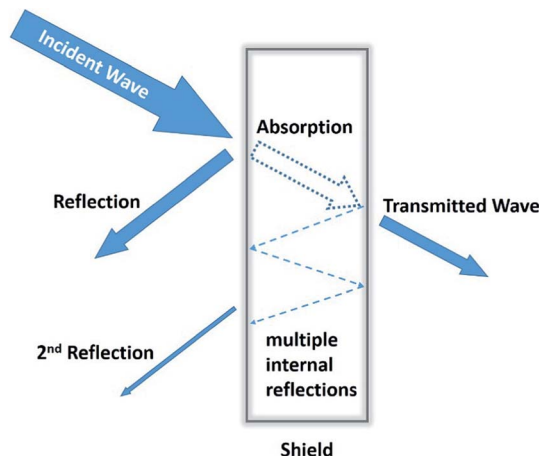


Fig. 1 Schematic of EMI shielding.

where P_i is the incident power and P_o is the transmitted power. When $SE_{\text{total}} \geq 10$ dB, SE_M can be negligible.

According to the transmission line theory,²⁵ the input impedance (Z_{in}) on the interface can be expressed as

$$Z_{\text{in}} = Z_0 \sqrt{\frac{\mu_r}{\epsilon_r}} \tanh\left(j \frac{2\pi f d}{c} \sqrt{\epsilon_r \mu_r}\right) \quad (2)$$

where Z_0 is the impedance of free space, μ_r is the complex permeability, $\mu_r = \mu' - j\mu''$, ϵ_r is the complex permittivity, $\epsilon_r = \epsilon' - j\epsilon''$, f is the frequency, d is the thickness of material, and c is the speed of light.

Thus, the reflection loss (RL) can be expressed as

$$RL(\text{dB}) = 20 \lg \left| \frac{Z_{\text{in}} - Z_0}{Z_{\text{in}} + Z_0} \right| \quad (3)$$

$$SE_A = -RL \quad (4)$$

For a material, the skin depth (δ) is the distance up to which the intensity of the electromagnetic wave decreases to $1/e$ of its original strength. It can be expressed as^{24,26}

$$\delta = \sqrt{\frac{2}{\mu_r \omega \sigma_s}} \quad (5)$$

According to electromagnetic theory, for electrically thick samples ($d > \delta$), frequency (ω) dependence of far field losses, reflection from the material surface (SE_R) can be expressed as^{24,26}

$$SE_R(\text{dB}) = 10 \lg \left(\frac{\sigma_s}{16\omega\mu'\epsilon_0} \right) \quad (6)$$

where $\sigma_s = \omega\epsilon_0\epsilon''$ is the frequency dependent conductivity,²⁷ ω is the angular frequency ($\omega = 2\pi f$) and ϵ_0 is the permittivity of the free space.

Results and discussion

The morphologies of the DBEDOT and PEDOT are shown in Fig. 2. After being heated at 80 °C for hours, the colorless

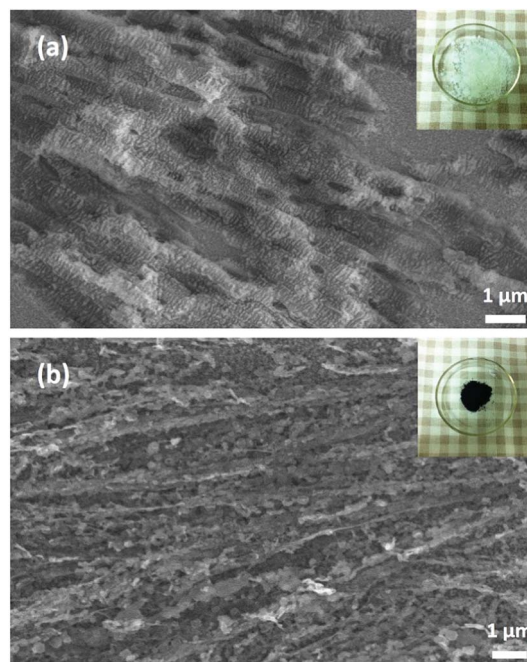


Fig. 2 Digital photos and FE-SEM images of DBEDOT (a) and SSP-PEDOT (b).

DBEDOT powder transformed into a dark blue material (PEDOT). SEM image of a higher magnification revealed a significant change in the surface morphology. The pure DBEDOT has a smooth surface but the surface of the PEDOT film exhibits a stripe-like microstructure, which might result from the formation of the polymer chain during the polymerization process.^{20,21}

To investigate the doping degree of Br in SSP-PEDOT, we performed XPS studies on SSP-PEDOT with different heating times. The XPS spectra with a heating time of 24 h are shown in Fig. 3. There are familiar peaks in each sample (see ESI†), which are characterized as O 1s, C 1s, S 2p and Br 3d. The elements C, O, S come from the SSP-PEDOT structure, and the element Br should be from doping the polymer chain during the SSP process. The atom% of Br are given in Table 1, and the 24 h

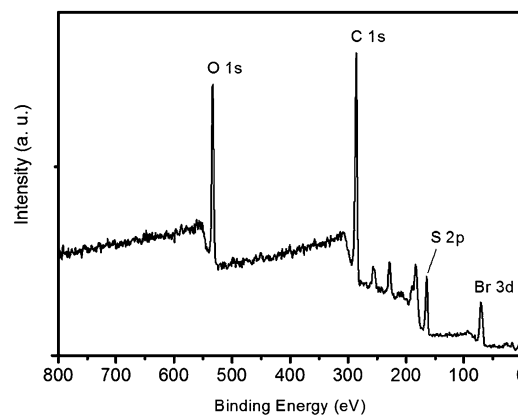


Fig. 3 XPS spectra of SSP-PEDOT with heating time of 24 hours.

Table 1 The atom% of Br in each sample

	1 h	2 h	4 h	8 h	12 h	24 h	48 h
Atom% of Br	9.793%	7.203%	6.165%	7.291%	6.467%	5.679%	6.524%

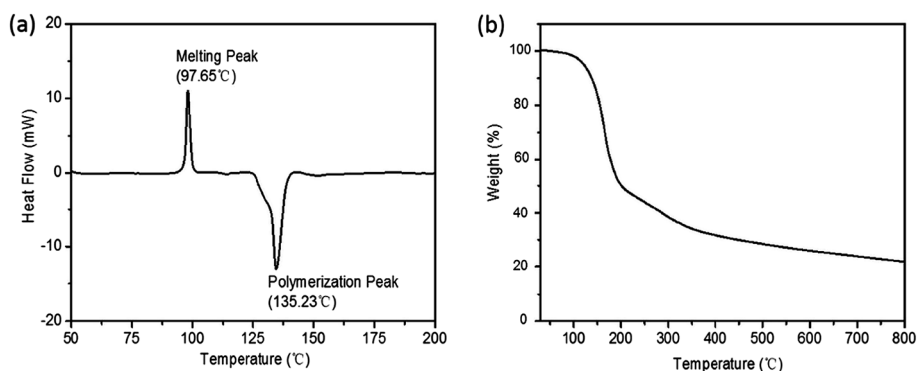
Table 2 Molecular weight of SSP-PEDOT with different heating times

Heating time	Mn	PDI
1 h	1070	1.02
2 h	1060	1.01
4 h	1050	1.02
8 h	1070	1.01
12 h	1040	1.01
24 h	1050	1.01
48 h	1080	1.01

sample has the lowest doping degree, which indicated that with this sample it is possible to obtain a well-defined polymer structure²⁰ and good conductivity. GPC studies showed that the SSP-PEDOT synthesized at different temperatures have similar molecular weights (M_n) with a relatively narrow polydispersity index (PDI) of around 1, as listed in Table 2. Thus, the DBEDOT monomer was polymerized in a short time and the volume of Br doping degree should contribute to the extended heating time.

When the monomer DBEDOT is heated at $10\text{ }^\circ\text{C min}^{-1}$, it exhibits an endothermic melting phenomenon. As we can see from Fig. 4a, the position of the melting peak is at $97.65\text{ }^\circ\text{C}$. The melting point results in an exothermic polymerization peak at $135.23\text{ }^\circ\text{C}$, which implies that polymer formation and doping occurs.²⁰ There is a huge weight loss during the heating process, which is close to the polymerization point (Fig. 4b). This phenomenon should be due to the volatility of elemental Br_2 during the SSP process. The TGA curve under atmosphere is similar with the nitrogen situation before $300\text{ }^\circ\text{C}$ (see ESI[†]), which gives the evidence that DBEDOT has the same polymerization process in inert gas and air. In addition, it is a quite suitable temperature ($80\text{ }^\circ\text{C}$) for SSP, which we have chosen in this experiment.

The electromagnetic energy absorption ability of SSP-PEDOT, as a kind of dielectric material, is related to complex permittivity (ϵ_r). In a coaxial wire analysis, a radiated wave undergoes shielding (reflection, absorption, and transmission) when the incident wave at a point i pass toward another point j , and these wave scattering values are expressed as S_{ji} . To probe further, ϵ_r of the dielectric material has been calculated from the experimental scattering parameters S_{11} (or S_{22}) and S_{21} (or S_{12}) using the standard Nicolson–Ross–Weir (NRW) algorithm.^{28,29} Real permittivity (ϵ') represents the charge storage (or dielectric constant), whereas imaginary permittivity (ϵ'') is a measure of dielectric loss. Therefore, we investigated the ϵ_r of SSP-PEDOT under different heating times. Fig. 5 shows the ϵ' and ϵ'' of the ϵ_r in the frequency range of 2–18 GHz. When the heating time is 1 or 2 hours, the ϵ' and ϵ'' of the SSP-PEDOT remains stable in the entire frequency range with a low value. According to the free electron theory, low conductivity would result in low permittivity.³⁰ It indicates that these two samples should have poor electromagnetic energy absorption ability. On increasing the heating, the ϵ' and ϵ'' of the SSP-PEDOT increased gradually initially, which implies that the conductivity has been improved during the heating process. The ϵ' remained stable before 12 GHz, and after that, it decreased with increasing frequency in varying degrees, which may be related to a resonance behavior that was reported before.³¹ The ϵ' is mainly associated with the amount of polarization occurring in the material, and the ϵ'' is related to the dissipation of energy.³² Thus, when a material has a high value of ϵ'' , it may have potential in electromagnetic energy absorption. The samples with the heating times of 4, 8, 12, 24 and 48 hours have obvious growth processes in the ϵ'' part, which we believe will benefit the electromagnetic energy absorption ability. In addition, there are vibration peaks at the range of 11–17 GHz in these samples, which shows that a strong dielectric loss can be found in this

Fig. 4 DSC and TGA curves of the DBEDOT at a heating scan of $10\text{ }^\circ\text{C min}^{-1}$ under nitrogen flow.

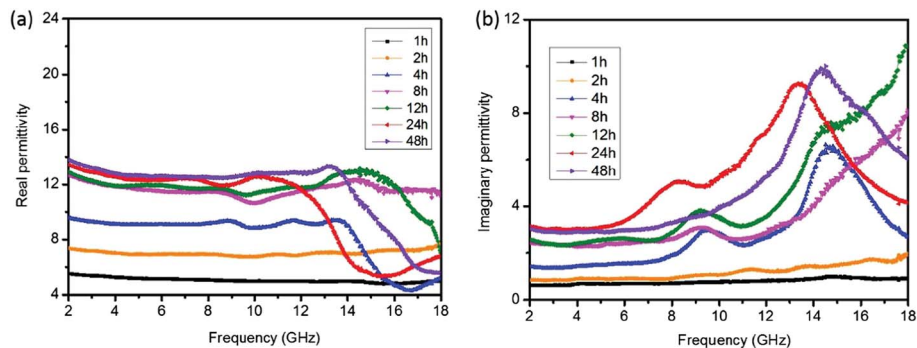


Fig. 5 Electromagnetic characteristics of SSP-PEDOT with different heating times in the 2–18 GHz range: (a) real part of complex permittivity and (b) imaginary part of complex permittivity.

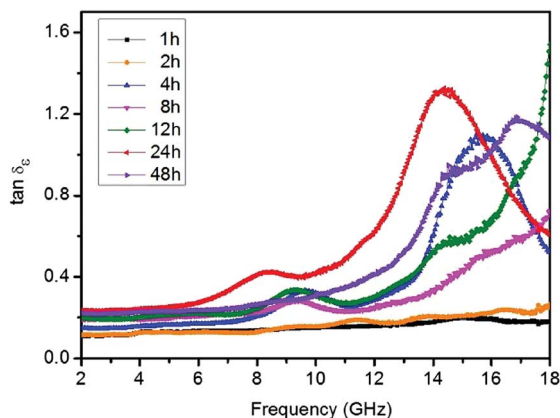


Fig. 6 Dielectric loss tangent ($\tan \delta_e$) of SSP-PEDOT with different heating times in the 2–18 GHz range.

area. However, it is still hard to explain which sample has the best ability of electromagnetic energy absorption. Therefore, we compared the dielectric loss tangent ($\tan \delta_e$), which is related to microwave attenuation in dielectric materials. It can be expressed as

$$\tan \delta_e = \frac{\epsilon''}{\epsilon'} \quad (7)$$

Fig. 6 shows the $\tan \delta_e$ of each sample, it is easy to find that SSP-PEDOT with heating for 24 hours has the maximum value

before 16 GHz. The relatively high values of ϵ'' and $\tan \delta_e$ implies that this sample has the best electromagnetic energy absorption ability, which should be attributed to such mechanisms as dominant dipolar polarization, interfacial polarization and associated relaxation phenomena.³³

According to the eqn (2) and (3) mentioned before, we calculated the RL of each sample using a self-written MATLAB program (see ESI†). The calculated results are shown in Fig. 7. It is not surprising that the samples of 1 h and 2 h have nearly no electromagnetic energy absorption ability because the values of ϵ_r and $\tan \delta_e$ explained this phenomenon. It is noted that the absorption value is related to the value of $\tan \delta_e$, it can be seen clearly that SSP-PEDOT with a heating time of 24 hours exhibited a maximum absorption of -50.1 dB at 11.2 GHz. The thickness of the sample is an important parameter related to the intensity and the position, as well as the frequency range of electromagnetic energy absorption. We chose the sample of 24 h and analyzed it in 1.5, 2.0, 2.5, 3.0 mm thicknesses to explore the influence of the sample thickness. With the growth of the sample thickness, it was obvious to find that the absorbing peaks shifted to a lower frequency. Each one has an absorbing range deeper than -10 dB (which means it can yield a 90% of microwave attenuation). The sample with 2 mm thickness not only has the maximum absorption value, but also the maximum bandwidth. In Fig. 7b, it can clearly be seen that this sample's bandwidth with the RL deeper than -10 dB is nearly 5.9 GHz (from 10.0 GHz to 15.9 GHz), which is better than that of oxidative PEDOT and the composite of PEDOT with graphene

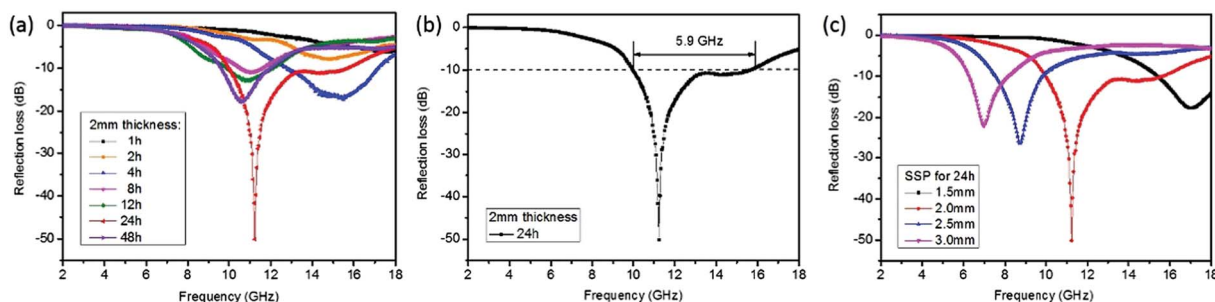


Fig. 7 Reflection loss curves for the (a) SSP-PEDOT with different heating times in 2 mm thickness, (b) SSP-PEDOT with a heating time of 24 hours in 2 mm thickness, (c) SSP-PEDOT with a heating time of 24 hours in different thicknesses in the frequency range of 2–18 GHz.

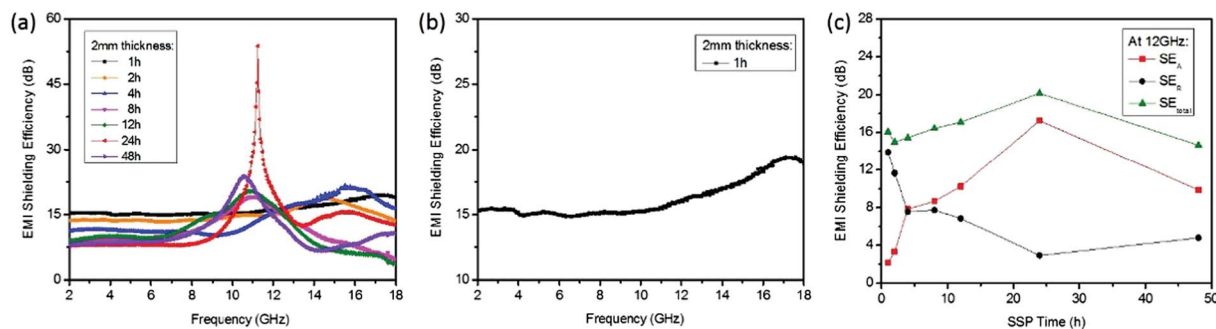


Fig. 8 (a) EMI SE of SSP-PEDOT with different heating times, (b) the best EMI SE of SSP-PEDOT with a heating time for 1 hour, (c) comparison of SE_{total} , SE_A , and SE_R at 12 GHz as a function of SSP-PEDOT.

(see ESI†). These results show that the SSP-PEDOT predicts good electromagnetic energy absorption ability in both low- and high-frequency bands.

Electromagnetic energy absorption is only a part of the ability for EMI shielding in a material, and therefore we also measured the ability of electromagnetic energy reflection for each sample, according to eqn (1), (4), and (5). The curves of SE_{total} for each sample are shown in Fig. 8a. From the frequency range of SE, we find that the sample of 4, 8, 12, 24, and 48 h, is highly related to their SE_A . Although the sample of 24 h has the maximum value of SE_{total} , it loses the SE out of the SE_A frequency range. On the contrary, the samples of 1 or 2 h have good SE in the entire frequency range, especially for sample of 1 h. In Fig. 8b, we clearly see that this sample has a $SE_{total} \geq 15$ dB from 2–18 GHz. The EMI shielding mechanism was investigated by plotting SE_{total} , SE_A and SE_R of each sample loading at 12 GHz (Fig. 8c). The shielding mechanism varied with the heating time, the value of SE_R decreased gradually, and the value of SE_A did the opposite. The sample of 1 h has the best SE, nearly 87% is contributed to the SE_R . It is worth noting that this SSP-PEDOT with different heating times have several applications in the EMI protection. For example, camouflage in military (using the electromagnetic energy absorption), and protection from electronic devices (using the EMI shielding).

Conclusion

In conclusion, a low cost, large frequency range material for electromagnetic energy absorption and EMI shielding has been successfully developed *via* a facile SSP at 80 °C for different heating hours using DBEDOT monomer as the starting material. The superior performance indicates that SSP-PEDOT is a promising material for EMI protection in military camouflage and electronic devices protection.

Acknowledgements

The work was financially supported by the National Natural Science Foundation of China (51021001). We also thank Dr P. Xu for help in XPS tests.

References

- 1 C. Y. Lee, H. G. Song, K. S. Jang, E. J. Oh, A. J. Epstein and J. Joo, *Synth. Met.*, 1999, **102**, 1346.
- 2 B. R. Kim, H. K. Lee, S. H. Park and H. K. Kim, *Thin Solid Films*, 2011, **519**, 3492.
- 3 Z. P. Chen, C. Xu, C. Q. Ma, W. C. Ren and H. M. Cheng, *Adv. Mater.*, 2013, **25**, 1296.
- 4 N. Li, Y. Huang, F. Du, X. B. He, X. Lin, H. J. Gao, Y. F. Ma, F. F. Li, Y. S. Chen and P. C. Eklund, *Nano Lett.*, 2006, **6**, 1141.
- 5 Y. Yang, M. C. Gupta, K. L. Dudley and R. W. Lawrence, *Nano Lett.*, 2005, **5**, 2131.
- 6 S. T. Hsiao, C. C. M. Ma, H. W. Tien, W. H. Liao, Y. S. Wang, S. M. Li and Y. C. Huang, *Carbon*, 2013, **60**, 57.
- 7 B. Shen, W. T. Zhai, M. M. Tao, J. Q. Ling and W. G. Zheng, *ACS Appl. Mater. Interfaces*, 2013, **5**, 11383.
- 8 H. R. Tantawy, D. E. Aston, J. R. Smith and J. L. Young, *ACS Appl. Mater. Interfaces*, 2013, **5**, 4648.
- 9 P. Saini, M. Arora, G. Gupta, B. K. Gupta, V. N. Singh and V. Choudhary, *Nanoscale*, 2013, **5**, 4330.
- 10 S. Varshney, A. Ohlan, V. K. Jain, V. P. Dutta and S. K. Dhawan, *Mater. Chem. Phys.*, 2014, **143**, 806.
- 11 P. B. Liu, Y. Huang and X. Sun, *ACS Appl. Mater. Interfaces*, 2013, **5**, 12355.
- 12 F. Jonas, G. Heywang, B. Gladbach, W. Schmidtberg, J. Heinze and M. Dietrich, US Patent no. 5,035,926, 1991.
- 13 F. Jonas and L. Schrader, *Synth. Met.*, 1991, **831**, 41.
- 14 L. B. Groenendaal, F. Jonas, D. Freitag, H. Pielartzik and J. R. Reynolds, *Adv. Mater.*, 2000, **12**, 481.
- 15 L. B. Groenendaal, G. Zotti, P. H. Aubert, S. M. Waybright and J. R. Reynolds, *Adv. Mater.*, 2003, **115**, 855.
- 16 M. Magat, *Polymer*, 1962, **3**, 449.
- 17 M. J. Cohen, A. F. Garito, A. J. Heeger, A. G. MacDiarmid, C. M. Mikulski, M. S. Saran and J. Kleppinger, *J. Am. Chem. Soc.*, 1976, **98**, 3844.
- 18 M. He, H. Okudera, A. Simon, J. Köhler, S. F. Jin and X. L. J. Chen, *Solid State Chem.*, 2013, **197**, 466.
- 19 M. He, H. Okudera and A. Simon, *Inorg. Chem.*, 2005, **44**, 4421.
- 20 H. Meng, D. F. Perepichka, M. Bendikov, F. Wudl, G. Z. Pan, W. J. Yu, W. J. Dong and S. Brown, *J. Am. Chem. Soc.*, 2003, **125**, 15151.

- 21 H. Meng, D. F. Perepichka and F. Wudl, *Angew. Chem., Int. Ed.*, 2003, **42**, 658.
- 22 G. A. Sotzing, J. R. Reynolds and P. J. Steel, *Chem. Mater.*, 1996, **8**, 882.
- 23 X. Yin, F. Wu, N. Q. Fu, J. Han, D. L. Chen, P. Xu, M. He and Y. Lin, *ACS Appl. Mater. Interfaces*, 2013, **5**, 8423.
- 24 N. F. Colaneri and L. W. Shacklette, *IEEE Trans. Instrum. Meas.*, 1992, **41**, 291.
- 25 Y. Naito and K. Suetake, *IEEE Trans. Microwave Theory Tech.*, 1971, **19**, 65.
- 26 A. P. Singh, P. Garg, F. Alam, K. Singh, R. B. Mathur, R. P. Tandon, A. Chandra and S. K. Dhawan, *Carbon*, 2012, **50**, 3868.
- 27 A. Ohlan, K. Singh, A. Chandra and S. K. Dhawan, *Appl. Phys. Lett.*, 2008, **93**, 053114.
- 28 A. M. Nicolson and G. F. Ross, *IEEE Trans. Instrum. Meas.*, 1970, **4**, 377.
- 29 W. B. Weir, *Proc. IEEE*, 1974, **62**, 33.
- 30 C. Wang, X. Han, P. Xu, X. Zhang, Y. Du, S. Hu, J. Wang and X. Wang, *Appl. Phys. Lett.*, 2011, **98**, 072906.
- 31 H. Zhang, A. J. Xie, C. P. Wang, H. S. Wang, Y. H. Shen and X. Y. Tian, *J. Mater. Chem. A*, 2013, **1**, 8547.
- 32 K. Singh, A. Ohlan, V. H. Pham, B. Balasubramanian, S. Varshney, J. Jang, S. H. Hur, W. M. Choi, M. Kumar, S. K. Dhawan, B. S. Kong and J. S. Chung, *Nanoscale*, 2013, **5**, 2411.
- 33 M. Zhou, X. Zhang, J. M. Wei, S. L. Zhao, L. Wang and B. X. Feng, *J. Phys. Chem. C*, 2011, **115**, 1398.